Neuron 50, 277–289, April 20, 2006 ©2006 Elsevier Inc. DOI 10.1016/j.neuron.2006.03.042

TRPA1 Contributes to Cold, Mechanical, and Chemical Nociception but Is Not Essential for Hair-Cell Transduction

Kelvin Y. Kwan,[1,*] Andrew J. Allchorne,[2] Melissa A. Vollrath,[1] Adam P. Christensen,[3] Duan-Sun Zhang,[1] Clifford J. Woolf,[2] and David P. Corey[1]

[1] Department of Neurobiology and Howard Hughes Medical Institute Harvard Medical School Boston, Massachusetts 02115

[2] Neural Plasticity Research Group Department of Anesthesia and Critical Care Massachusetts General Hospital and Harvard Medical School 13th Street Building 149 Charlestown, Massachusetts 02129

[3] Program in Neuroscience Harvard Medical School Boston, Massachusetts 02115

Summary

TRPA1, a member of the transient receptor potential (TRP) family of ion channels, is expressed by dorsal root ganglion neurons and by cells of the inner ear, where it has proposed roles in sensing sound, painful cold, and irritating chemicals. To test the in vivo roles of TRPA1, we generated a mouse in which the essential exons required for proper function of the *Trpa1* gene were deleted. Knockout mice display behavioral deficits in response to mustard oil, to cold (~0° C), and to punctate mechanical stimuli. These mice have a normal startle reflex to loud noise, a normal sense of balance, a normal auditory brainstem response, and normal transduction currents in vestibular hair cells. TRPA1 is apparently not essential for hair-cell transduction but contributes to the transduction of mechanical, cold, and chemical stimuli in nociceptor sensory neurons.

Introduction

TRPA1 is a member of the transient receptor potential (TRP) family of ion channels. Originally identified as a protein overexpressed in liposarcoma cell lines (Jaquemar et al., 1999), TRPA1 (or ANKTM1) is similar to other TRP channels in having six putative transmembrane domains with a putative pore-forming helix between the fifth and sixth transmembrane domains (Clapham, 2003). Like many other TRPs, it has ankyrin repeats in the N-terminal region. However, TRPA1 is unique among mammalian TRPs in having as many as 17 ankyrin repeats. TRPN1 (or NOMPC), a proposed mechanosensory transducer in flies (Walker et al., 2000), has 29 ankyrin repeats but is present only in genomes of lower vertebrates and invertebrates.

*Correspondence: kelvin_kwan@hms.harvard.edu

Interest in TRPA1 has come from a search for the molecular basis for several different senses. To identify the mechanically gated transduction channel of vertebrate hair cells, Corey et al. (2004) used in situ hybridization to screen all mouse TRP channels for expression in the inner ear and found TRPA1 message in neonatal hair-cell sensory epithelia. TRPA1 mRNA in the utricle appeared during development at E16, the day before hair cells become mechanically responsive, and antibodies to TRPA1 labeled the tips of mouse and frog hair-cell stereocilia, the site of mechanotransduction. Zebrafish were found to have two *TRPA* genes, now denoted *TRPA1a* and *TRPA1b*. Morpholino knockdown of TRPA1a expression in zebrafish embryos decreased cytoplasmic loading of styryl dyes such as FM1-43, which pass through intact hair-cell transduction channels (Meyers et al., 2003). Microphonic recordings from the inner ear, produced by the hair-cell transduction currents, were also reduced in zebrafish TRPA1a morphants. In mice, knockdown of TRPA1 expression in embryonic hair cells using two different small interfering RNAs largely abolished hair-cell transduction currents. Thus, TRPA1 was proposed as a candidate for the hair-cell transduction channel (Corey et al., 2004).

TRPA1 has been implicated in pain sensation as well. It is activated by allyl isothiocyanate (mustard oil) and by other pungent chemicals including allicin (from garlic), cinnamaldehyde (cinnamon), methysalicylate (wintergreen), eugenol (cloves), and gingerol (ginger) (Jordt et al., 2004; Bandell et al., 2004; Bautista et al., 2005; Macpherson et al., 2005), all of which elicit a painful burning or pricking sensation. TRPA1 is expressed in small-diameter neurons of the trigeminal and dorsal root ganglia (DRGs), mostly in a subset of cells that express TRPV1 but not TRPM8 (Story et al., 2003; Bautista et al., 2005; Kobayashi et al., 2005). TRPV1 is thought to sense painfully hot temperatures. TRPM8 is activated by cool temperatures and by chemicals such as menthol and icilin that feel cool when applied to the skin (McKemy et al., 2002; Peier et al., 2002). Because TRPM8 is activated below 23ºC, which feels cool but not painfully cold (Morin and Bushnell, 1998), another channel is thought to mediate cold nociception. Story et al. (2003) reported that TRPA1, when expressed in CHO cells and assayed with Ca^{2+} imaging, is activated by temperatures below ~15ºC, temperatures that in humans elicit burning, aching, or pricking pain (Morin and Bushnell, 1998). Thus, TRPA1 was proposed to mediate the sensation of cold pain, an idea supported by reduced cold hyperalgesia with TRPA1 knockdown in vivo (Story et al., 2003; Obata et al., 2005). However, Jordt et al. (2004) found that most mustard oil-responsive trigeminal ganglion neurons were not sensitive to cold (5ºC), which may mean either that TRPA1 is not a cold pain sensor or that additional ion channels can be activated by mustard oil in trigeminal ganglia.

The prolonged latency of activation by these pungent compounds, and by carbachol when TRPA1 is cotransfected with the muscarinic acetylcholine receptor, suggest that TRPA1 channel opening can be mediated by

second messengers. Moreover, Δ^9-tetrahydrocannabinol (THC), which binds to the CB1 receptor, also activates TRPA1 in a heterologous system, as does bradykinin, an inflammatory peptide acting through its G protein-coupled receptor, B2R (Jordt et al., 2004; Bandell et al., 2004). Recently, Bautista et al. (2006) have deleted the *Trpa1* gene in mice, and find that knockout animals lack sensitivity to mustard oil and to bradykinin but not to painful cold or mechanical stimuli.

These studies suggest that TRPA1 may be an intermediate where several different modalities converge to elicit pain, and that plants like mustard, garlic, and cinnamon have—for their protection—evolved chemicals that target this pathway.

TRPA genes also occur in invertebrate genomes; there are four in *Drosophila*, for instance. The *Drosophila* homolog closest to TRPA1 is sensitive to heat above ~27ºC, and knockdown of dmTRPA1 abolishes thermotaxic behavior in fly larvae (Viswanath et al., 2003; Rosenzweig et al., 2005). Another *Drosophila* TRPA, dubbed *painless*, is expressed by polymodal nociceptors, is located in their branched sensory endings, and is involved in sensing both noxious hot temperatures (55ºC) and intense mechanical stimuli (Tracey et al., 2003). Thus, a common theme for TRPA1 function is nociception, but the specific sensory modalities in mammals, especially the sensation of noxious cold, remain controversial.

To understand the role of TRPA1 in auditory and vestibular function as well as temperature, chemical, and mechanical sensation, we generated mice lacking a functional *Trpa1* gene. Surprisingly, TRPA1 is not necessary for hair-cell transduction, but mice lacking TRPA1 have reduced sensitivity to mustard oil and bradykinin, as well as to painful cold and mechanical stimuli.

Results

Generation of *Trpa1*$^{-/-}$ Mice

We designed a targeting vector to delete in mice the exons encoding for the pore domain of TRPA1. The S5 and S6 transmembrane domains and the pore loop that contains the selectivity filter of TRPA1 were replaced with a cassette containing an internal ribosome entry site (IRES) with a human placental alkaline phosphatase gene (PLAP) and a polyadenylation sequence (Figures 1A and 1B). Deletion of the pore-forming region of TRPA1 renders the channel nonconducting, and the resulting mutant allele forms a bicistronic mRNA transcript containing the 5′ end of TRPA1 followed by an independently translated human placental alkaline phosphatase gene. Since a truncated product of the *Trpa1* gene might still be produced and cause unwanted side effects, an endoplasmic reticulum (ER) retention signal encoded by the amino acid sequence KDEL and a stop codon were placed in frame with the exon before the IRES PLAP cassette. Any potential truncated product of *Trpa1* produced from the bicistronic transcript should be sequestered in the ER. Sequestration of the potential truncated TRPA1 fragment was confirmed by expressing the truncated fragment with the ER retention signal in human epithelial kidney (HEK) cells (data not shown).

Transfection of the linearized targeting vector into murine embryonic stem (ES) cells resulted in the deletion of one of the *Trpa1* alleles. Two independent ES cell lines carrying the targeted *Trpa1* mutation were injected into blastocysts to generate germline chimeric males. Mating of male chimeras with C57Bl/6J or B6129PF2/J produced heterozygote animals that were subsequently intercrossed. Southern blot analysis of DNA from progeny of heterozygote matings shows that the mutant allele has properly recombined into the *Trpa1* locus (Figure 1C). Matings of heterozygote animals resulted in a total of 227 animals with a ratio of 1.1:1.9:0.9 wild-type to heterozygote to mutant animals, a ratio close to the expected Mendelian ratio.

To ensure that the transcript was no longer present in mutant animals, mRNA from DRGs was harvested from mice of each genotype. Amplification of the transcript by RT-PCR, in a region after the site of deletion, indicated that *Trpa1* message was present in wild-type and heterozygote animals but absent in *Trpa1*$^{-/-}$ mice, suggesting that there was no functional TRPA1 protein in knockout animals (Figure 1D). Using primers that lie in the deletion site, quantitative RT-PCR confirmed that the *Trpa1* transcript was absent in *Trpa1*$^{-/-}$ mice and was reduced by 50% in heterozygote animals (Figure S2 in the Supplemental Data available with this article online).

Auditory and Vestibular Sensitivity

TRPA1 has been proposed as a candidate for the hair-cell transduction channel (Corey et al., 2004). We asked whether *Trpa1*$^{-/-}$ mice exhibit hearing and balance defects, if hair cells in *Trpa1*$^{-/-}$ mice contain functional transduction channels, and—if so—if the properties of transduction and adaptation are altered relative to wild-type mice.

Behavioral Tests

Adult wild-type and *Trpa1*$^{-/-}$ mice displayed a normal Preyer reflex, flicking their ears when startled with a loud sound, suggesting that auditory function was normal. *Trpa1*$^{-/-}$ mice swam normally, could maintain balance on a rotating rod, and could walk along the top of a thin wall, indicating normal vestibular function (data not shown).

Auditory Brainstem Response

To evaluate the function of the cochlea at different auditory frequencies, we measured auditory brainstem responses (ABRs) of wild-type, heterozygous, and *Trpa1*$^{-/-}$ mice, evoked with short tone pips. The overall ABR thresholds were nearly identical at all frequencies from 4 to 45.3 kHz, differing only at 32 kHz, where if anything the *Trpa1*$^{-/-}$ mice were more sensitive (Figure 2A).

AM1-43 Accumulation in Utricle and Cochlea

The fluorescent styryl dyes, FM1-43 and its fixable analog AM1-43, rapidly enter hair cells through their transduction channels, offering a simple test of functional transduction (Gale et al., 2001; Meyers et al., 2003). We dissected cochleas and utricles from wild-type, heterozygous, and *Trpa1*$^{-/-}$ mice and bathed them for 2 min in dye before washing, fixing, and colabeling for actin. By this measure, most hair cells possessed functional transduction channels, in both cochleas and utricles of both mutant and wild-type mice (Figures 2B and 2C).

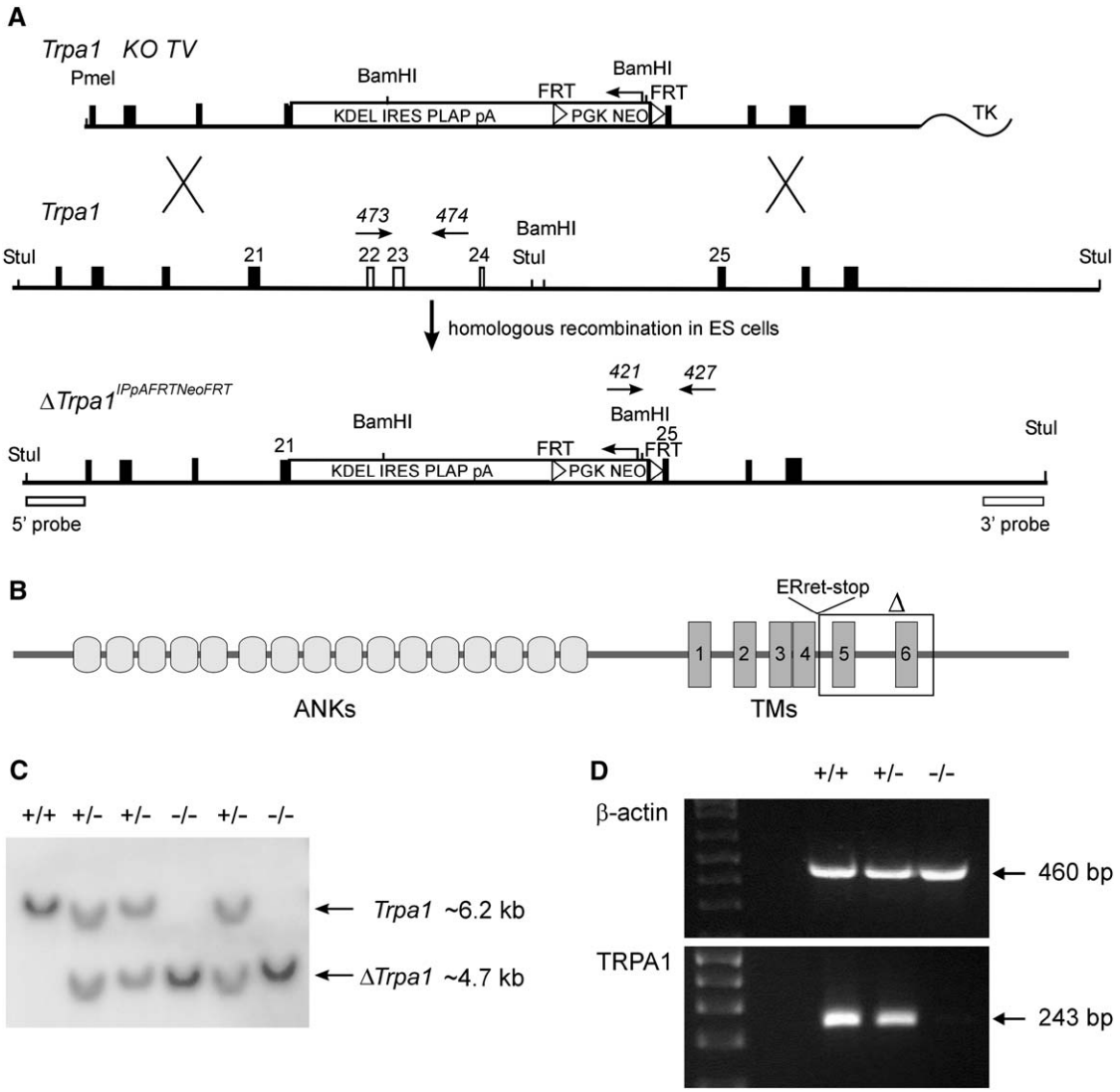

Figure 1. Production of *Trpa1* Knockout Mice

(A) Relevant regions of the targeting vector, the endogenous *Trpa1* locus, and the expected *ΔTrpa1* allele. Black boxes denote exons in the depicted *Trpa1* genomic region, and exons labeled 21–25 encode a region encompassing the S5 and S6 transmembrane domains. Only restriction sites relevant for genotyping are depicted. Proper homologous recombination of the targeting vector to the *Trpa1* locus results in the replacement of several exons with the KDEL IRES PLAP pA and PGK Neo cassettes. Primers 473/474 and 421/427 (arrows) were used for PCR amplification of the wild-type and mutant *Trpa1* allele, respectively. The 5′ and 3′ probes used in genotyping are shown as boxes.

(B) Domain structure of the TRPA1 protein, indicating ankyrin repeats and transmembrane domains. The region enclosed by the box (Δ), which included the pore domain between S5 and S6, was deleted and replaced with an ER retention signal followed by a stop codon.

(C) Representative results of genotyping wild-type, heterozygote, and mutant mice by Southern blot analysis using the 3′ probe.

(D) RT-PCR using total RNA derived from DRG of wild-type, heterozygote, and mutant mice. β-actin was used as a positive control. *Trpa1* mRNA was not detected in the mutant animals but was observed in wild-type and heterozygote animals.

We could not detect a difference in AM1-43 loading between the different genotypes.

Transduction Current

The best measure of transduction channel function is single-cell recording of currents elicited with calibrated deflection of hair bundles. We measured whole-cell transduction currents in mouse utricular hair cells from *Trpa1*$^{-/-}$ and *Trpa1*$^{+/-}$ littermate mice, aged P2 to P6, with genotype unknown to the experimenter. The properties of transduction and adaptation did not differ significantly between *Trpa1*$^{-/-}$ and *Trpa1*$^{+/-}$ hair cells (Figures 2D and 2E), and were similar to those reported previously for wild-type mice (Vollrath and Eatock, 2003). The average maximal transduction current, I_{max}, for ten *Trpa1*$^{-/-}$ and five *Trpa1*$^{+/-}$ hair cells was 129 ± 18 and 131 ± 27 pA, respectively. Other measures of transduction and adaptation (resting open probability, operating range, time constant of decay, and extent of adaptation at steady state; Table 1) were normal. A rebound at the termination of negative deflections (Figure 2E) suggested that climbing adaptation to negative steps was normal. To assess adaptation more completely, we presented a series of test deflections before and during an adapting step and measured

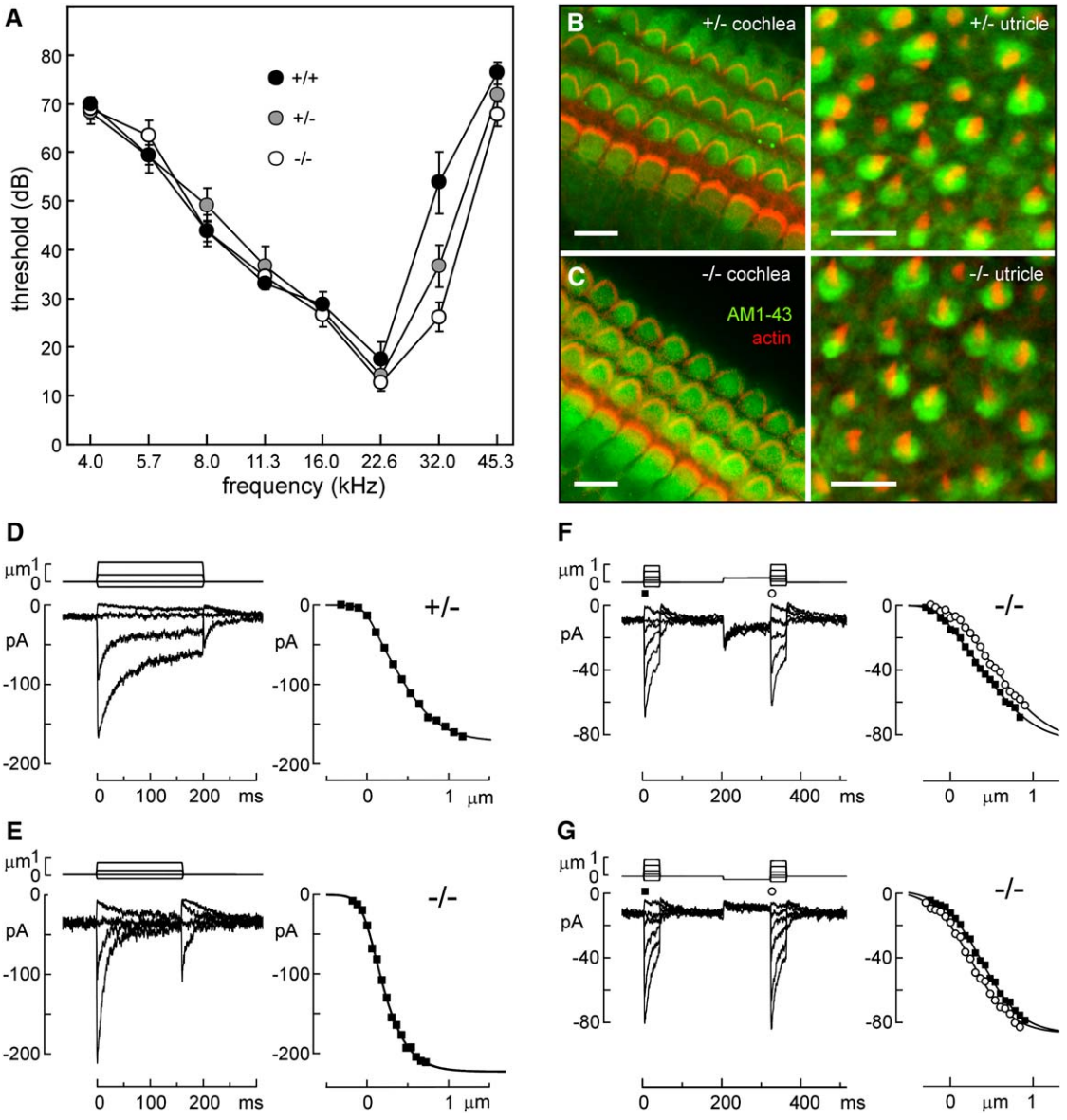

Figure 2. Auditory and Vestibular Function in Knockout Mice

(A) Auditory brainstem-evoked response. Thresholds were measured for 5 ms tone pips of frequencies from 4 to 45 kHz. Knockout mice hear normally. Mean ± SEM; n = 10 (+/+), n = 8 (+/−), n = 9 (−/−).

(B) AM1-43 accumulation in heterozygote cochlea and utricle. Organs were incubated in 5 μM AM1-43 for 2 min, then washed and fixed. Hair cells with functional transduction channels are labeled with this procedure. Phalloidin labeling of actin revealed hair bundles. Nearly all cells were labeled in wild-type cochleas and utricles. Scale bar is 10 μm.

(C) AM1-43 accumulation in knockout cochleas and utricles. Nearly all cells were labeled.

(D) Transduction currents (left) and the measured activation curve (right) in a heterozygote utricular hair cell. The stimulus is shown above the currents. Transduction and adaptation are typical for this preparation.

(E) Transduction currents and activation curve in a knockout utricular hair cell. Adaptation was faster and the activation curve steeper in this cell than in wild-type cells, but on average knockout hair cells were normal (Table 1).

(F) Adaptation to a maintained positive deflection in a knockout hair cell, measured as a shift of the activation curve. Responses to test steps presented before (filled squares) and at the end (open circles) of a 0.24 μm, 120 ms adapting step were fitted with a three-state Boltzmann relation (Equation 2). The activation curve shifted by 0.18 μm, so extent was 75%. Adaptation appears normal.

(G) Adaptation to a maintained negative deflection in a knockout hair cell. Adaptation appears normal.

the resulting shift of the activation curve. *Trpa1*$^{-/-}$ hair cells had normal adaptation in response to both positive and negative adapting steps (Figures 2F and 2G). Taken together, these data suggest that hair cells in *Trpa1*$^{-/-}$ mice are normal. We cannot rule out more subtle defects.

Chemical Sensitivity

Mice lacking TRPA1 were then tested for oral sensitivity to the irritating or painful sensation elicited by mustard oil. Mice were allowed access to water for 3 hr/day, and water consumption was measured. No significant difference in normal water consumption was found

Table 1. Properties of Transduction and Adaptation

	I_{max} (pA)	P_0 (%)	Operating Range (nm)	τ_A (ms)	Extent (%)	n
wild-type	155 ± 16	14 ± 1	749 ± 59	30 ± 2	76 ± 3	31
Trpa1$^{+/-}$	131 ± 27	7 ± 1	841 ± 192	28 ± 8	79 ± 6	5
Trpa1$^{-/-}$	129 ± 18	12 ± 3	812 ± 71	37 ± 7	71 ± 5	10

Values are mean ± SE. P_0 is percent of current activated at rest; operating range is 10%–90% of I_{max}; τ_A is adaptation time constant measured from current decay for a half-maximal displacement; extent of adaptation measured from curve fitted to decay. Wild-type values from Vollrath and Eatock (2003).

among wild-type, heterozygote, and *Trpa1*$^{-/-}$ mice. After several days, mustard oil was added to the water in different concentrations. At the highest concentration, 100 mM, wild-type, and heterozygote mice would not drink the water at all, whereas *Trpa1*$^{-/-}$ mice consumed over a third of the normal amount (Figure 3A). Because mustard oil might also activate other channels expressed by trigeminal nociceptors, we tried lower concentrations. At all concentrations, *Trpa1*$^{-/-}$ mice consumed more mustard oil-containing water than did wild-type mice, and heterozygote animals displayed an intermediate phenotype (Figure 3B).

Olfactory receptors may also contribute to the perception of mustard oil in this test. Therefore, we injected 20 μl of a 75 mM mustard oil solution into the plantar surface of a hind paw and recorded the amount of time the mouse spent licking, flinching, or flicking the affected paw. *Trpa1*$^{-/-}$ mice demonstrated a decrease in this pain behavior compared to their wild-type counterparts (Figure 3C). Injection of a mineral oil control did not elicit a significant behavioral response from the animals. As in the oral sensitivity test, heterozygote mice had an intermediate phenotype, suggesting a gene dosage effect.

Because *Trpa1*$^{-/-}$ mice showed some avoidance of mustard oil-containing water, we asked whether TRPA1 is the sole mediator of mustard oil sensitivity of DRG neurons. We cultured dissociated cells from wild-type and mutant DRGs and loaded them with Fluo-4 to detect Ca^{2+} entry upon chemical stimulation. TRPA1 is expressed in a subset of TRPV1-expressing DRG neurons in the mouse (Kobayashi et al., 2005). To identify TRPV1-expressing cells, capsaicin (3 μM) was applied to DRG cultures first. In wild-type mice, 31% ± 4% of cells (mean ± SEM; n = 12) responded to capsaicin with a rise in Ca^{2+} fluorescence, and 25% ± 5% responded to capsaicin in *Trpa1*$^{-/-}$ mice, which was not significantly different (Figures 3E–3G). We applied mustard oil (10 μM) 80 s later. The number of mustard oil-sensitive cells was significantly lower in knockouts (wild-type, 23% ± 4%; knockout, 12.5% ± 2.5%; $p < 0.01$; Figures 3E–3G). Moreover, there were almost no cells responding to both drugs in the knockout (wild-type, 13% ± 2%; knockout, 0.7 ± 0.3%; Figure 3G). Thus, there are still mustard oil-sensitive cells in *Trpa1*$^{-/-}$ mice (Figure 3F), but these are not the TRPV1-expressing cells where most TRPA1 is expressed. The remaining response to mustard oil is apparently mediated by another receptor expressed in other neurons.

Thermal Nociception

Heat

To study the involvement of TRPA1 in sensing noxious temperatures, animals of all three genotypes were subjected to hot temperatures known to elicit a nociceptive behavioral response. We placed mice on a hot plate at 50ºC, 52ºC, or 55ºC, temperatures in the high range for TRPV1 and TRPV2 (Patapoutian et al., 2003), and recorded the latency to initial nocifensive behavior. As the temperature was increased, the latency decreased, but there were no observable differences between the *Trpa1*$^{+/+}$, *Trpa1*$^{+/-}$, and *Trpa1*$^{-/-}$ animals (Figure 4A). Although no difference was expected, this indicates that pain avoidance mechanisms are intact in *Trpa1*$^{-/-}$ mice.

Cold

A Peltier cooler was used to generate a cold surface maintained at 0ºC ± 1ºC, which is substantially below the apparent threshold of ~10ºC for cold pain in rats (Allchorne et al., 2005). A mouse was placed on the plate, and the number of paw withdrawal responses during 5 min was used as an integrated index of the nociceptive response to cold (Figure 4B). *Trpa1*$^{-/-}$ animals were significantly less responsive to noxious cold than their wild-type and heterozygote littermates ($p < 0.0004$).

We also applied a drop of acetone to the dorsolateral surface of a hind paw to cause evaporative cooling, which evokes a brief period of shaking and elevation of the paw in mice (Carlton et al., 1994; Choi et al., 1994). *Trpa1*$^{-/-}$ mice showed reduced sensitivity to the cooling sensation compared to wild-type and heterozygote mice ($p < 0.02$) (Figure 4C).

For both the cold plate and acetone tests, the difference between wild-type and knockout mice was larger for females than for males (Figure S1).

Mechanical Nociception

Mechanical sensitivity was determined by probing the plantar surface of the left hind paw with calibrated von Frey filaments. *Trpa1*$^{-/-}$ mice were less sensitive to the transient punctate mechanical stimuli relative to their wild-type littermates, measured either as the frequency of responses to forces between 0.04 and 2.0 g or as threshold (Figures 5A and 5B). At higher forces, *Trpa1*$^{-/-}$ mice consistently responded about half as often as wild-type littermates, indicating a deficit in sensitivity to suprathreshold stimuli. Heterozygote animals had an intermediate phenotype.

Because von Frey filaments can activate both Aδ and C fiber high-threshold rapidly adapting cutaneous mechanoreceptors to produce a pricking pain, we also used the Randall-Selitto test, in which blunt pressure is applied to a paw and the force increased until it elicits a vocalization or a withdrawal response. This test should assess mechanical pain elicited by slowly adapting cutaneous and subcutaneous high-threshold mechanoreceptors, which are predominantly C fibers. Although the test is well established for rats, the majority of mice in our tests displayed no active

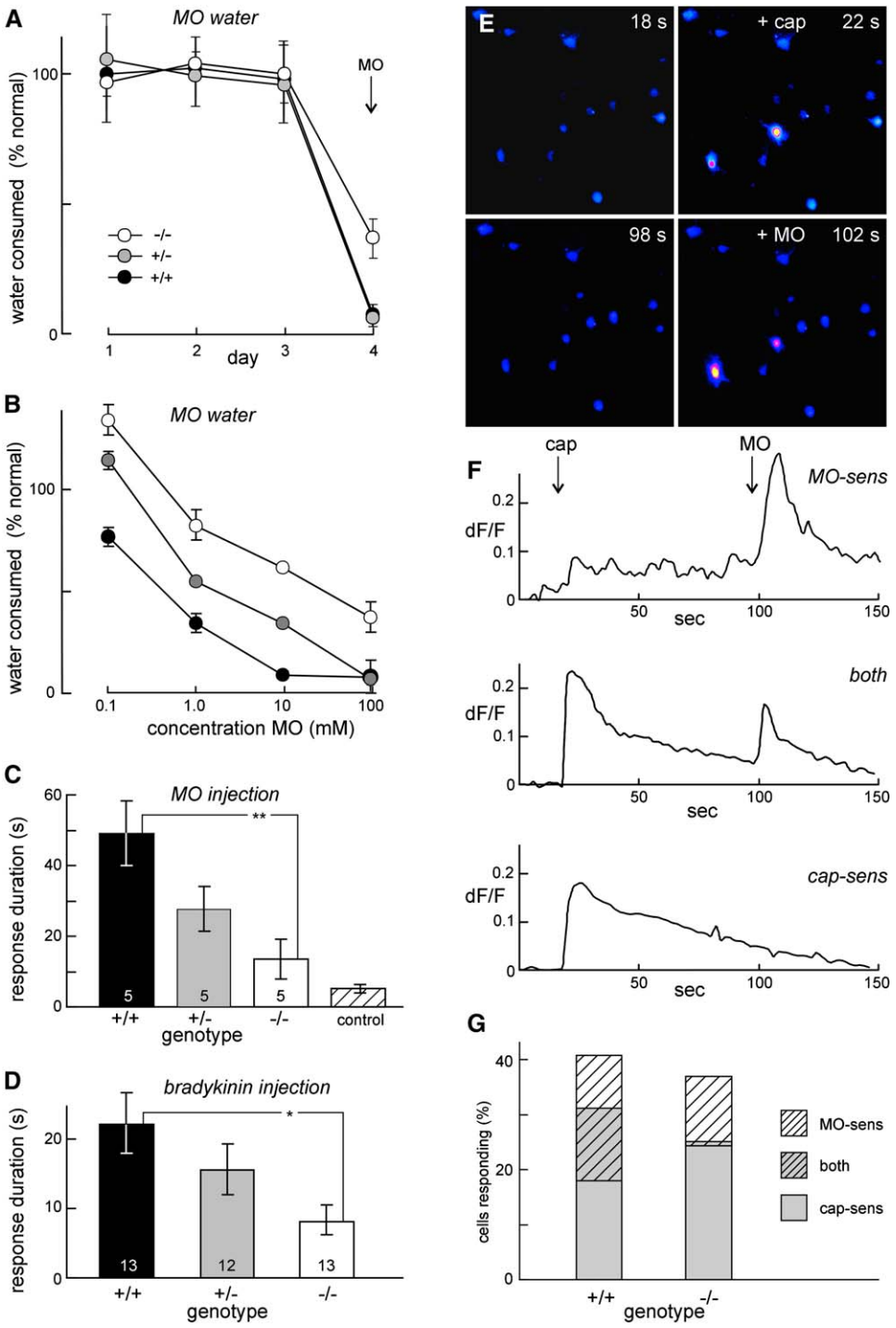

Figure 3. Responses of Knockout Mice to Capsaicin and Mustard Oil

(A) Oral aversion to mustard oil (MO; allyl isothiocyanate). Water-deprived mice were allowed to drink from a sample bottle for 3 hr/day, and the volume consumed was measured. On days 1–3, the water was normal and consumption was ~2 ml; on day 4 it contained 100 mM mustard oil. Wild-type and heterozygote mice would not drink it on day 4; knockout mice still consumed ~40% of normal. Mean ± SEM; n = 5 mice of each genotype.

(B) Concentration dependence of oral aversion to MO. Shown is consumption on the test day relative to previous days as a function of MO concentration. Mean ± SEM; n = 5 of each genotype, except n = 1 for 1 mM. Knockout mice were consistently less deterred than wild-type by MO; heterozygote mice were consistently intermediate in phenotype.

(C) Pain response to subcutaneous mustard oil. MO (20 μl of 0.75% or 75 mM) was injected into the left hind footpad, and the duration of pain responses (licking, lifting) was measured. Knockout mice apparently felt less pain (**p = 0.01); heterozygotes had intermediate responses. Five animals of each genotype.

(D) Pain response to subcutaneous bradykinin. In another set of animals, bradykinin (300 ng in 0.9% saline) was injected into the left hind footpad. Knockout mice showed reduced pain-like behavior (*p = 0.014). Males and females; numbers as shown.

response up to the test limit of 300 g. Nevertheless, fewer knockout mice showed a pain response than wild-type, and the average threshold was higher in knockouts than in wild-type (241 ± 12 g [wild-type] versus 274 ± 7 g [knockout]; mean ± SEM; p = 0.01).

Bradykinin-Induced Pain and Hyperalgesia

Subcutaneous bradykinin causes inflammatory pain, and it has been proposed to activate TRPA1 via the B2R G protein-coupled receptor (Story et al., 2003). To test the role of TRPA1 in inflammatory pain, 300 ng of bradykinin in 10 μl saline was injected into the plantar surface of the mouse paw. After the injection, all three groups of mice displayed a flinching and licking behavior indicative of an irritant action of the peptide. We measured the cumulative time spent with the paw elevated during 15 min. Wild-type mice spent almost three times as long tending to the affected paw as *Trpa1* knockout mice (22.1 ± 4.5 s versus 8.1 ± 2.2 s; p = 0.014), suggesting that bradykinin was less painful in knockout mice. Heterozygote animals displayed an intermediate effect (Figure 3D).

Bradykinin injected peripherally also causes hypersensitivity to mechanical stimuli. To determine whether this mechanical hyperalgesia is mediated by TRPA1, mice were tested with von Frey hairs for mechanical sensitivity 2 hr after injection. All animals had reduced thresholds following bradykinin, but wild-type mouse thresholds were reduced 5-fold, whereas the reduction in knockout mice was not significant (Figure 5B).

Spared Nerve Injury

Animals were treated to produce the spared nerve injury model of peripheral neuropathic pain, by ligation of the tibial and common peroneal nerves leaving the sural nerve intact, and were tested 7 and 14 days after surgery. After spared nerve injury, all three groups showed mechanical thresholds lowered by more than tenfold (Figure 5C). TRPA1 is apparently not involved in mechanical hypersensitivity after peripheral nerve injury. These observations are consistent with the idea that such mechanical hypersensitivity (tactile allodynia) is mediated by low-threshold, large, myelinated, nonpeptidergic Aβ fibers that normally sense innocuous stimuli such as touch, hair movement, or gentle pressure (Campbell et al., 1988; Koltzenburg et al., 1994) and do not express TRPA1 (Kobayashi et al., 2005). The presurgery mechanical pain sensitivity (Figure 5C) showed the same reduction in threshold in knockout and heterozygotes as that seen in a separate cohort of naive animals (Figure 5A), and pre-bradykinin injection (Figure 5B).

Discussion

TRPA1 Is Not an Essential Component of Hair-Cell Transduction

Despite strong evidence that TRPA1 mediates hair-cell mechanotransduction (Corey et al., 2004), mice lacking TRPA1 do not have any detectable vestibular or auditory defects. The mice showed no defects in balance or in the noise-evoked startle reflex. Mutant mice had normal hearing, as assessed by auditory brainstem recordings. Hair cells in both cochlea and utricle had functioning transduction channels based on the accumulation of AM1-43. Moreover, neonatal vestibular hair cells from *Trpa1*$^{-/-}$ mice displayed transduction currents in response to bundle deflections that were normal in terms of current amplitude, operating range and position, and time course and extent of adaptation.

Is TRPA1 the hair-cell mechanotransduction channel early in development? The knockdown with morpholinos in zebrafish was tested in early stage larvae at 50–60 hr postfertilization, almost as soon as hair cells appeared, and the siRNA inhibition in mice was done in embryonic utricles (Corey et al., 2004). Perhaps TRPA1 is only used in developing hair cells. In the knockout mice, however, transduction currents were normal when tested at postnatal day 2, not long after transduction appears at E17. It seems unlikely that TRPA1 is used from E17 to P0, and then replaced by another channel postnatally.

Is TRPA1 in just a subset of transduction channels in hair cells? Transduction channels are thought to be present at both ends of the tip links (Denk et al., 1995), but the structure of the tip link is not identical at both ends, showing two branches at the upper end and three or more at the lower end (Kachar et al., 2000), and so the molecular components at either end also may not be identical. Perhaps TRPA1 is only present at one end of the tip link. However, the total amplitudes of transduction currents were normal in *Trpa1*$^{-/-}$ mice, inconsistent with the idea that half the channels are missing.

In other studies with gene deletion in mice, function can remain if compensatory genes are upregulated. It is possible that another TRP channel in hair cells, perhaps even another subunit of the transduction channel, can compensate for the loss of TRPA1. However, no other TRP channel in mammalian genomes has the unique architecture of TRPA1 with its extended N terminus of ankyrin repeats. If this domain is essential for transduction, there is not another channel that can substitute. It seems clear from the phenotype of the *Trpa1*$^{-/-}$ mice that TRPA1 is not, at least, an essential component of the adult mouse hair-cell transduction channel. Still to be determined is why inhibiting its expression with morpholinos in developing zebrafish or with siRNAs in mouse cultures reduces hair-cell mechanotransduction currents (Corey et al., 2004).

TRPA1 Participates in Sensitivity to Mustard Oil

Behavioral aversion for mustard oil was greatly reduced in *Trpa1*$^{-/-}$ mice, suggesting the involvement of TRPA1 in sensing the painful stinging and burning caused by mustard oil. At the lowest concentration of mustard oil tested (0.1 mM), the mutant mice consumed slightly

(E) Responses of dissociated DRG neurons to capsaicin (cap) and mustard oil (MO). Representative images acquired at 18, 22, 98, and 102 s are shown. Application of capsaicin (3 μM; at time 20–26 s) caused an increase in Fluo-4 fluorescence in some cells, mustard oil (10 μM; at time 100–110 s) increased fluorescence in others, and some cells responded to both.

(F) Fluorescence intensity (as fractional change) in three representative cells: a MO-sensitive cell (top), a capsaicin-sensitive cell (bottom), and a cell responsive to both (middle). The start of capsaicin and MO delivery is indicated by arrows.

(G) Proportion of DRG neurons responding to MO and to capsaicin, from wild-type and knockout animals. In knockout animals, capsaicin-sensitive neurons were largely insensitive to MO.

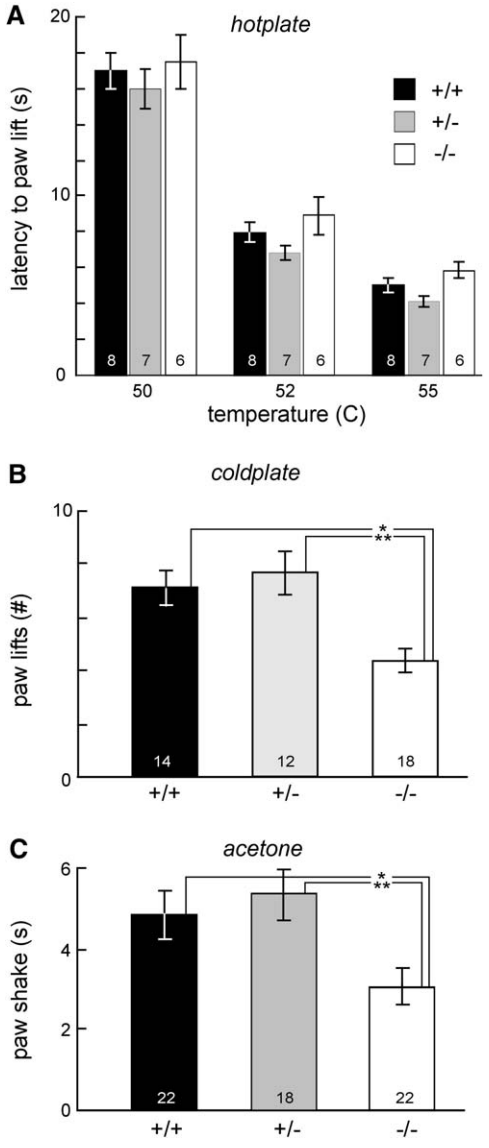

Figure 4. Thermal Pain in Knockout Mice

(A) Hotplate. Mice were placed on a hotplate maintained at 50ºC, 52ºC, or 56ºC, and the time before a hind paw was lifted was measured. There was no significant difference in latency between knockout, heterozygote and wild-type mice, but all showed decreasing latency with increasing temperature. Mean ± SEM; number of animals of each genotype as shown; three trials each.

(B) Cold plate. Mice were placed on a cold plate maintained at 0ºC, and the number of paw lifts during 5 min was counted. Knockout mice showed significantly fewer paw lifts than did wild-type or heterozygote (*$p < 0.0004$; **$p < 0.0002$). Animal numbers as shown for each genotype; four trials each; not separated by sex.

(C) Acetone cooling. A drop of acetone was placed on a hind paw, causing evaporative cooling, and the duration of paw lifting or shaking was measured. Knockout mice showed significantly shorter pain-like behavior than did wild-type (*$p < 0.02$; **$p < 0.004$). Animal numbers as shown; not separated by sex.

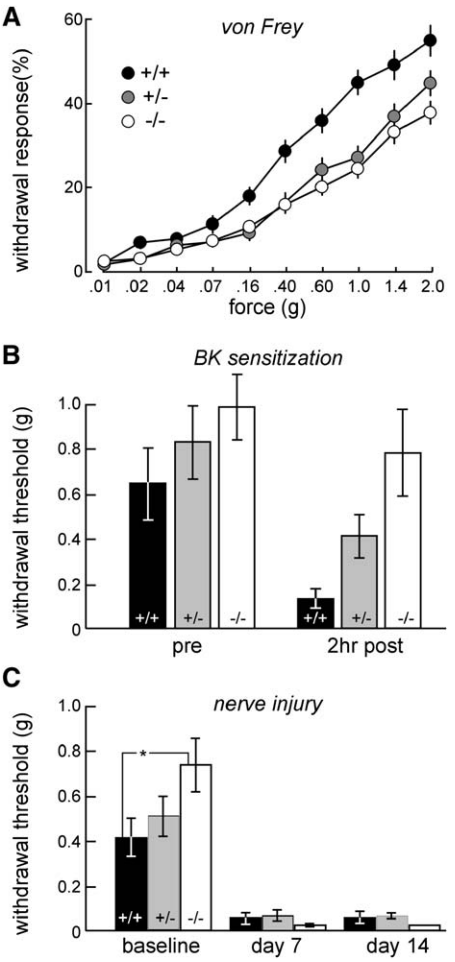

Figure 5. Mechanical Pain in Knockout Mice

(A) Plantar withdrawal response, measured with calibrated von Frey hairs for ten presentations at each force. Fourteen animals (seven males and seven females) of each genotype were tested; there was no significant difference between sexes, so results were pooled. Mean ± SEM.

(B) Plantar withdrawal threshold, measured before and 2 hr after injection of bradykinin into footpad. Bradykinin increased the sensitivity of wild-type mice to von Frey stimulation, reducing thresholds by 5-fold, but in knockout mice thresholds were not significantly reduced. Thirteen animals of each genotype.

(C) Plantar withdrawal thresholds measured before, and at 7 and 14 days after spared nerve injury. Knockout mice showed significantly higher thresholds than wild-type (*$p = 0.03$) before nerve injury. Loss of TRPA1 did not protect from development of hypersensitivity.

more water than the baseline. The reason for increased consumption is not clear, but pungent compounds such as garlic, yellow mustard, and wasabi, which contain TRPA1-activating compounds (Bautista et al., 2005), are used as flavor enhancers by humans. Diminished noxious sensation of mustard oil in *Trpa1*$^{-/-}$ mice may unmask a preference for pungent compounds. At higher concentrations, mustard oil was partially aversive in *Trpa1*$^{-/-}$ mice, suggesting that the mice may smell or otherwise sense the mustard oil using a different nociceptive chemotransduction receptor. Indeed, our calcium imaging experiments in dissociated DRG neurons showed that, while TRPV1-positive cells in the *Trpa1*$^{-/-}$ mice were no longer sensitive to mustard oil, another population of cells remained responsive; these may express another receptor for mustard oil.

Trpa1$^{-/-}$ mice injected with mustard oil into the hind paw showed significantly less pain-like behavior, as assayed by licking or lifting the paw. TRPA1 does seem

necessary for mediating the normal painful sensation elicited by mustard oil.

TRPA1 Participates in Bradykinin-Induced Pain and Mechanical Hypersensitivity

Trpa1 knockout mice appeared much less sensitive to bradykinin injected in a paw, suggesting that activation of this channel mediates the acute pain of bradykinin. In addition, bradykinin-induced mechanical hypersensitivity, tested 2 hr after injection, was largely missing in knockout mice. Both consequences are expected if TRPA1 mediates the inflammatory pain caused by bradykinin.

TRPA1 Participates in the Response to Painful Cold Temperatures

Trpa1$^{-/-}$ mice showed no difference from wild-type or heterozygote mice in their sensitivity to noxious hot stimuli (50ºC–55ºC), indicating that pain response pathways are intact. They did show reduced sensitivity to intense cold (0ºC). Similarly, when acetone evaporation was used to elicit a cooling sensation, a reduced sensitivity was observed in mutant animals. The reduction in cold sensitivity was larger for female knockouts than for males (Figure S1). Sex differences in response to painful stimuli and the increased sensitivity of female rodents have been well documented; these differences have been partly attributed to the influence of gonadal steroid hormones (Berkley, 1997; Fillingim and Ness, 2000; Craft et al., 2004).

While the cold pain deficit in knockouts is consistent with a role for TRPA1 as a primary sensor for severe cold in mouse DRG (Story et al., 2003), its potential role as a cold sensor may be more complicated. In cultured rat DRGs, two distinct populations of neurons have been reported to respond to cold: one group of cells is activated at innocuous cold temperatures and is menthol sensitive; these neurons presumably express TRPM8. The second group is not sensitive to menthol but is also not activated by icilin or mustard oil, agonists of TRPA1, suggesting that TRPA1 is not expressed in this group and that the cold sensor is an unknown protein (Babes et al., 2004). There is a possible third cold-sensitive group, which is sensitive to both mustard oil and menthol (Babes et al., 2004; Reid, 2005). In cultured trigeminal neurons from rat, a population of cells sensitive to mustard oil and most likely expressing TRPA1 was identified. Only about 4% responded to a 5ºC cold stimulus, but these were also menthol sensitive (Jordt et al., 2004). Similarly, about 16% of TRPA1-positive neurons in rat DRG also express TRPM8 (Kobayashi, et al., 2005), based on in situ hybridization. Thus, TRPA1 may function together with TRPM8, either as a primary sensor or as a downstream mediator, in a subset of nociceptors sensitive to colder temperatures.

Mustard oil evokes a sharp burning or stinging pain in human subjects (Reeh et al., 1986; Handwerker et al., 1991; Koltzenburg et al., 1992). In contrast to stimuli of ~15ºC, which elicit a cool sensation that can be interpreted as unpleasant or even painful, intense cold stimuli (~0ºC) produce a burning, stinging, pricking sharp pain (Morin and Bushnell, 1998) not unlike that evoked by mustard oil, which is consistent with the idea that TRPA1 is involved in signaling intense cold pain.

Regardless of mechanism, the behavioral deficit in *Trpa1*$^{-/-}$ mice indicates that TRPA1 contributes to the burning cold pain elicited by very cold temperatures.

TRPA1 Contributes to Sensitivity to Mechanical Pain

TRPA1-deficient mice displayed a deficit in sensing noxious punctate cutaneous mechanical stimuli, which elicit a pricking pain: they had higher thresholds than those of wild-type mice and had consistently and significantly reduced responses to a series of suprathreshold stimuli. It is possible that TRPA1 is part of a high-threshold mechanotransduction complex in the peripheral sensory system, perhaps directly gated by mechanical force. The participation of a *Drosophila* TRPA, *painless*, in mechanical nociception suggests an evolutionarily conserved role for this branch of the TRP family (Tracey et al., 2003; Corey et al., 2004). Several biophysical features of TRPA1 are reminiscent of the high-threshold mechanoreceptor, which is a nonselective cation channel with a reversal potential around 0 mV that can be blocked by gadolinium, similar to some characteristics of heterologously expressed TRPA1 (Hu et al., 2006). Ruthenium Red, a TRP channel blocker, can also inhibit the high-threshold mechanotransducer in DRG neurons. It is equally possible that a different mechanosensitive protein leads indirectly to the activation of TRPA1, which then provides the depolarizing current for spike initiation. Fast measurements of mechanically elicited currents in TRPA1-expressing cells should reveal whether the transduction current is too fast for a second messenger.

In addition, pricking pain can be evoked by activation of Aδ mechano-nociceptors, but these do not express TRPA1 (Kobayashi et al., 2005), so it is likely that while TRA1 may contribute to mechanotransduction in some C fiber nociceptors, another high-threshold mechanotransducer exists as well.

While this manuscript was in review, a paper from Bautista et al. (2006) appeared that describes the phenotype of another TRPA1 knockout mouse. Although the phenotypes of these two lines are generally similar, Bautista et al. did not observe a deficit in cold pain sensitivity or in mechanical pain. The reasons for these differences are unclear but may lie in the test specifics. Bautista et al. only used male mice for cold behavioral tests, whereas we observed the greatest difference in cold sensitivity in females. They focused on mechanical pain thresholds, whereas we observed the greatest difference in higher-force response rates. The population of neurons for calcium imaging from adult DRG neurons in our study is different from the newborn trigeminal neurons used by Bautista et al. (2006). During the early postnatal period, the neurotrophins are still specifying the functional identity of sensory neurons (Lewin and Mendell, 1993). The distinction in the population of cells is highlighted by the difference in the number of TrkA-positive neurons in early postnatal animals and adult animals (McMahon et al., 1994; Molliver et al., 1997). It will be important to resolve these issues, to help understand whether TRPA1 can be a primary sensory receptor channel or serves exclusively as a downstream integrator of diffusible messengers.

Experimental Procedures

Construction of *Trpa1* Knockout Mouse

Targeting Vector

Sequences flanking the exons encoding the S5 and S6 transmembrane domains were selected as homologous arms for the *Trpa1* knockout targeting vector. The 3.4 kb 5′ homologous arm (31186–34574 bp, using the first base pair of the *Trpa1* start codon as 1 bp in the genomic *Trpa1* sequence), followed by a KDEL sequence and a stop codon, was generated using polymerase chain reaction (PCR) with E14 ES cell DNA as template. A 3.4 kb 3′ homologous arm (42921–46336 bp) was amplified by PCR. An IRES PLAP pA reporter was inserted between the homologous arms along with a PGKNeo cassette flanked by FRT sites (Gene Bridges GmbH, Dresden, Germany) for positive selection. PLAP (placental alkaline phosphatase) is a GPI-linked membrane protein located on the extracellular surface, so antibody staining or chromogenic development of cells expressing PLAP allows for molecular identification of TRPA1-expressing cells. A thymidine-kinase cassette was inserted after the 3′ homologous arm for negative selection (Figure 1). The *Trpa1* IPpA PGKNeoFRT KO targeting vector was linearized with PmeI, phenol-chloroform extracted, and transfected into E14 ES cells (Simpson et al., 1997).

Targeted Disruption of Murine Trpa1

Murine E14 ES cells were transfected with 50 μg of linearized *Trpa1* IPpA PGKNeoFRT KO targeting vector. Cells were allowed to recover for 24 hr before selection in media containing 300 μg/ml of G418 and 2 μM ganciclovir (Invitrogen Corp., Carlsbad, CA). DNA samples were prepared from ES cells, initially screened for proper homologous recombination of both arms by PCR, and confirmed by Southern blot hybridization using radiolabeled probes that lie in regions outside of the targeting vector. The 5′ probe was generated by amplifying a fragment spanning 25083–26080 bp of the *Trpa1* genomic sequence and TA cloning it into a pCRII vector (Invitrogen Corp., Carlsbad, CA). The 3′ probe spanning 41345–42407 bp was similarly generated. Mouse genomic tail DNA was cleaved with either NheI and BamHI for annealing to the 5′ probe or StuI and BamHI for the detection with the 3′ probe. Restriction digests were electrophoresed on a 0.6% agarose 1X TAE gel and transferred onto Nytran N+ membrane (Amersham Biosciences, Piscataway, NJ) for Southern blot analysis.

Two ES cell clones containing the appropriate crossover events were injected into C57Bl/6 blastocysts to generate chimeric animals. Male chimeras capable of transmitting the disrupted *Trpa1* allele were selected and crossed with female C57Bl/6J or B6129P1/F2J mice. F1 progeny from these crosses were genotyped for the mutant allele using primer pairs oligo 473 5′-TCCTGCAAGGGTGATTGCGT TGTCTA-3′ and oligo 474 5′-TCATCTGGGCAACAATGTCACCTG CT-3′ for the wild-type allele. Oligo 421 5′-CCTCGAATCGTGGATCC ACTAGTTCTAGAT-3′ and oligo 427 5′-GAGCATTACTTACTAGC ATCCTGCCGTGCC-3′ are used to amplify a novel junction created in the *Trpa1* deletion allele. $Trpa1^{+/-}$ heterozygotes were then intercrossed to produce $Trpa1^{-/-}$ mutant mice.

Detection of Trpa1 *Transcript*

Mice of the appropriate genotypes were sacrificed, and DRGs were obtained from these animals. The DRGs were immediately placed in Tri Reagent (Ambion Inc., Austin, TX), homogenized by forcing the tissue and Tri Reagent through a 20 gauge needle several times followed by disruption through a 25 gauge needle using a 3 ml syringe, and extracted for total RNA as described by the manufacturer. A poly-dT primer was used for the reverse transcription reaction in conjunction with Moloney murine leukemia virus reverse transcriptase (MMLV RT) (BD Bioscience, San Jose, CA) to generate DNA as template for PCR amplification. Primers that are spanned by introns were designed to amplify murine β-actin (5′-GGCCCAGAGCAAGAG AGGTATCC-3′ and 5′-ACGCACGATTTCCCTCTCAGC-3′) and *Trpa1* (5′-ACAAGAAGTACCAAACATTGACACA-3′ and 5′-TTAACTGCG TTTAAGACAAAATTCC-3′).

For real-time RT-PCR, cDNA was synthesized using both oligo dT and random hexamers using the Advantage RT for PCR kit (BD Bioscience, San Jose, CA). The cDNA was diluted to 50 μl, and 5 μl of cDNA was used as template for PCR amplification. Primer pairs 400 5′-AGGTGATTTTTAAAACATTGCTGAG-3′ and 401 5′-CTCGATA ATTGATGTCTCCTAGCAT-3′ were used to detect the *Trpa1* transcript. Similarly, primer pairs 380 5′-GGCCCAGAGCAAGAGAGGT ATCC-3′ and 381 5′-ACGCACGATTTCCCTCTCAGC-3′ were used to amplify the β-actin transcript for normalization of the total mRNA amounts, with diluted cDNA (2.5 μl) as template. PCR reactions were set up by combining 0.12 μM final concentration of each primer pair, the appropriate amount of cDNA, and 12.5 μl of 2× SYBR Green supermix, and adjusted to a final volume of 25 μl with H_20 (Bio-Rad, Hercules, CA). The reaction was initially denatured at 95 C for 3 min, followed by 40 cycles of 30 s of denaturation, 30 s of annealing, and 45 s of extension on a MJ Research thermal cycler equipped with a Chromo4 detector. The fluorescence and analysis was done using the Opticon Monitor version 2 analysis software. Linear regression to determine the PCR efficiency for the *Trpa1* primers was determined, and relative amounts of transcripts were calculated as described by Ramakers et al. (2003).

Inner Ear Behavioral Tests

The Preyer (ear flick) reflex was elicited with 19.8 kHz, 96 dB sound from a source positioned about 30 cm from the mouse and assessed visually. Balance was tested by assessing ability to swim in deep water (mice with inner ear dysfunction tumble rapidly), to walk along the top of a 2 mm thick wall, and to maintain position on a 12 mm rotating rod.

Auditory Brainstem Recording

Mice were anesthetized with 100 mg/kg ketamine and 20 mg/kg xylazine (Henry Schein, Melville, NY). Platinum needle electrodes (Grass Telefactor, West Warwick, RI) were placed at the vertex and the mastoid, with a ground near the tail. Tucker-Davis System 3 instrumentation (Tucker-Davis Technologies, Alachua, FL) was used to generate the stimuli and acquire the evoked response. Tone pips (5 ms; 0.5 ms rise time) were presented through a closed field speaker at 25 s^{-1} at each frequency. Sound pressure level was varied in 5 dB steps from 10 to 90 relative dB. After acquisition and digitization, evoked potential wave forms were visually inspected to obtain a threshold value.

AM1-43 Dye Accumulation

Mouse utricles and cochleas (P4) were dissected as for physiology, below. At this age, the tectorial membrane is not fully formed, and protease was not required to remove it. Utricles and cochleas were treated with 5 μM FM1-43 or AM1-43 (Invitrogen Corp., Carlsbad, CA) for 2 min, then washed for 2 min. Tissues treated with FM1-43 were then viewed with a confocal microscope (Zeiss LSM510). Tissues treated with AM1-43 were fixed with 4% formaldehyde for 2 hr at room temperature and washed with PBS, and then hair bundles were labeled with Alexa Fluor 647 phalloidin. Images shown are maximum value projections of four to five images taken at 2 μm intervals, near the apical surface for actin and just below the apical surface for dye.

Hair-Cell Physiology

Preparation

Semi-intact preparations of the mouse utricle were made as described previously (Rüsch and Eatock, 1996; Vollrath and Eatock, 2003). Briefly, utricles of early postnatal mice (P2–P6) were exposed by opening the otic capsule, bathed for 20 min in standard extracellular solution (below) with 100 μg/ml protease type XXIV (Sigma, St. Louis, MO, St. Louis, MO) to facilitate removal of the otolithic membranes, and then dissected out and viewed on an upright microscope (Axioskop FS; Zeiss, Oberkochen, Germany) with a water immersion objective (63×) and differential interference contrast optics, all at 22°C–24°C. The extracellular solution for dissection and perfusion contained 144 mM NaCl, 0.7 mM NaH_2PO_4, 5.8 mM KCl, 1.3 mM $CaCl_2$, 0.9 mM $MgCl_2$, 5.6 mM D-glucose, 10 mM HEPES-NaOH, vitamins and minerals as in Eagle's MEM (pH 7.4, ~320 mmol/kg). The recording pipette contained 140 mM KCl, 0.1 mM $CaCl_2$, 10 mM EGTA-KOH, 3.5 mM $MgCl_2$, 2.5 mM Na_2ATP, 5 mM HEPES-KOH, 0.1 mM Li-GTP, 0.1 mM Na-cAMP (pH 7.4, ~300 mmol/kg).

Recording

Pipettes (3–5 MΩ) were pulled from R6 glass (Garner Glass, Claremont, CA). Hair-cell transduction currents were recorded in the whole-cell voltage-clamp mode, at −64 mV, with an Axopatch 200B amplifier. Stimulus waveforms were controlled by pClamp 9.0

software (Axon Instruments, Foster City, CA), and responses were digitized using a Digidata 1322A (Axon Instruments). Data analysis and fitting were done with Origin 6.0 (Microcal Software, Northampton, MA).

Stimulation

Transduction currents were elicited by deflecting hair bundles with a stiff probe. Borosilicate pipettes (1–2 μm tip; Sutter Instrument Co., San Rafael, CA) driven by a piezoelectric stimulator were brought into contact with the short edge of the hair bundle. Stimulus rise time (~1 ms; 10%–90% rise time) was measured with a photodiode; resonance was avoided by filtering the driving signal. Stimulus "creep" was less than 10% (Corey and Hudspeth, 1980).

Stimulus Protocols and Data Analysis

The decay of the transduction current during step deflections of the bundle was fitted with a single-exponential function.

$$I(t) = Ae^{-t/\tau_A} + I_{SS} \quad (1)$$

I is current, t is time, A is the amplitude of the exponential term, τ_A is the time constant of adaptation, and I_{SS} is the current level at steady state. To calculate the percent decay of the transducer current, I_{SS} was taken from the exponential fit for the steady-state current. I(X) relations were fitted with second-order Boltzmann functions:

$$I(X) = \frac{I_{max}}{1 + e^{A_2(P_2 - X)}\left(1 + e^{A_1(P_1 - X)}\right)} \quad (2)$$

A_1 and A_2 are constants that determine the steepness of the function, and P_1 and P_2 are constants that set the position of the function along the x axis. From the Boltzmann fits of I(X) relations, we measured the resting open probability, P_0, and the operating range corresponding to 10%–90% of I_{max}. To compare adaptation between cells, we used stimuli that evoked half-maximal activation of the transducer current.

Calcium Imaging

DRGs were dissected out of adult mice in Hank's balanced salt solution without Ca^{+2} or Mg^{+2} (HBSS; Invitrogen Corp., Carlsbad, CA), treated with 20 units/ml papain (Worthington Biochemicals) and 5 mM DL-cysteine (Sigma, St. Louis, MO) for 20 min at 37ºC. Enzyme solution was removed, and the ganglia were incubated with 3 mg/ml collagenase and 4 mg/ml dispase (Roche Diagnostics Corp., Indianapolis, IN) in HBSS at 37ºC for 20 min. The tissue was then mechanically triturated using fire-polished glass pipettes in L-15 medium (Invitrogen Corp., Carlsbad, CA) supplemented with 5 mM HEPES at pH 7.4. Cells were plated onto poly-D-lysine- and laminin-coated cover slips in D-MEM/F12 containing 10% FBS, 0.5 mM penicillin/streptomycin, 100 ng/ml NGF, and 2 ng/ml GDNF (Invitrogen Corp., Carlsbad, CA). DRG neurons were studied 16–36 hr after plating.

For dye loading, cells were incubated in HBSS containing Ca^{+2}, Mg^{+2} (HBSS+), and 2 μM Fluo-4 AM ester for 20 min at 37ºC, rinsed with HBSS+, and allowed to incubate for 20 min for complete deesterification of the Fluo-4 AM ester. HBSS+ and 3 μM capsaicin or 10 μM allyl-isothiocyanate (mustard oil; Sigma, St. Louis, MO) was flowed into the chamber using a Valvelink 8 pressurized flow system (Automate Scientific, Inc., San Francisco, CA) with a perfusion pen at 1.5 psi for 6 s and 10 s, respectively. Fluo-4 fluorescence was visualized with a 20× air objective (Zeiss) on an inverted microscope using a FITC filter set and acquired with a cooled CCD camera (Spot Flex, Diagnostic Instruments, Sterling Heights, MI); fluorescent images were collected every 2 s. To assess changes in fluorescence intensity, images 2–10 s after application of capsaicin and images 2–20 s after application of MO were compared to fluorescent images 2 s before application, using ImageJ (National Institutes of Health). Fluorescence intensity was pseudocolored with a color gradient in Adobe Photoshop.

Chemical Nociception Assay

Oral Aversion

Mice were allowed to drink from a measured water source for 3 hr each day but were otherwise water deprived. For 3 days, water was unadulterated; on the fourth day, it contained mustard oil (allyl isothiocyanate) at a concentration of 0.1, 1.0, 10, or 100 mM. Water containing mustard oil was sonicated with a Sonifier 250 (Branson Ultrasonics, Danbury, CT) using a microtip at setting 6 for 30 s to ensure emulsification of the solution.

Subcutaneous Injection

Mustard oil (Sigma, St. Louis, MO) (0.75% or 75 mM) was injected (20 μl) into the left hind footpad. Pain was assessed by paw lifts and licks, and the duration of such behavior was measured over a 5 min period.

Thermal Nociception Assay

Heat

Mice were placed on a hot plate analgesia meter (Stoelting Co., Wood Dale, IL) with surface temperature maintained at 50ºC, 52ºC, or 55ºC ± 1ºC. The latency before the first brisk lift or stamp of a hind paw was recorded (Suter et al., 2003). Immediately after the initial reaction, the trial was halted and the mice were removed from the hot plate. Animals were rested at least 10 min between each hot plate trial. Each trial started at the lower temperature and progressed toward hotter temperatures.

Cold

A Peltier-cooled cold plate, including a temperature controller and heat sink (TECA, Chicago, IL), was surrounded with a clear plastic barrier that restricted the test animal to an area of 8 cm W × 14 cm D × 14 cm H. A temperature probe (SPER Scientific, Scottsdale, AZ) was used to calibrate the surface temperature of the plate over a full range of temperatures (−5ºC to 25ºC). Mice were placed on a 0 ± 1ºC cold plate, and pain was assessed by counting the number of brisk left hind paw lifts during a 5 min period (Allchorne et al., 2005).

Mechano-Nociception Assays

For von Frey filaments, mice were placed in a 2 in cubicle made of wire mesh. Animals were habituated in the cubicles for 30 min/day for 3–7 days. For thresholds, von Frey hair tests were done using calibrated filaments (0.008–2 g; Stoelting Co., Wood Dale, IL), starting with the stiffest. Various regions of the plantar surface of the mouse left hind foot were subjected to each filament eight times at 1/s, with the filament positioned perpendicular to the plantar portion of the paw and pressed until a perceptible bend was observed, only when the mouse was not moving. Two out of eight paw withdrawals was a positive response for threshold. Over the whole force range, the number of paw withdrawals for each force was expressed as a percentage (Pertin et al., 2005).

For the Randall-Selitto test, mice were suspended in a restraining sling. They were habituated for 20 min/day for 2 days before testing. A blunt tip (0.7 mm) probe coupled to a digital force sensor (Model 2500, IITC Life Science, Woodland Hills, CA) was pressed against a paw until pain was signified by a withdrawal or vocalization, and the force required was recorded. Forces were not applied beyond 300 g, to avoid tissue damage.

Bradykinin Injection

After testing with thermal, chemical, and mechanical stimuli (three trials each), mice were treated with 300 ng of bradykinin (Sigma, St. Louis, MO) in 0.9% saline (10 μl), and the cumulative time spent licking or flicking the injected paw over a 15 min period was recorded. Two hours after injection, the mice were tested again for hyperalgesia.

Spared Nerve Injury

Unilateral spared nerve injury was done by exposing the sciatic nerve in the thigh region of the mouse, cutting and ligating the tibial and common peroneal nerves, and leaving the remaining sural nerve intact (Decosterd and Woolf, 2000). Animals were subjected to testing at 7 days and at 14 days after lesioning, in the plantar region of the left hind foot that is innervated by the sural nerve.

Animal Protocols

All experiments were approved by the Animal Care Committee of the Massachusetts General Hospital or Harvard Medical School and carried out according to the ethical guidelines of the International Association for the Study of Pain (Zimmermann, 1983).

Statistical Analysis

The genotypes of the mice were blinded to the experimenters for all the behavioral experiments. A single-factor ANOVA was used for all statistical measures of behavior.

Supplemental Data

The Supplemental Data include two supplemental figures and can be found with this article online at http://www.neuron.org/cgi/content/full/50/2/277/DC1/.

Acknowledgments

We thank Tam Thompsen, Yiping Zhou, and Lina Du for ES cell advice and blastocyst injections; Gui-Lan Yao and Bruce Bean for help with DRG dissection; Lisa Goodrich for the pTT0 plasmid with the IRES PLAP pA cassette; Michael Deans for advice on murine E14 ES cell culture and on generation of *Trpa1* mutant mice; Paul Niksch for dissecting mouse cochleae; Joe Corey for vestibular testing; and Stéphane Maison for technical advice on auditory brainstem recordings. We are also grateful for advice and comments from members of the Woolf laboratory. Supported by NIH grants NS-039518 and NS-038253 (to C.J.W.) and DC-00304 (to D.P.C.). D.P.C. is an Investigator and K.Y.K. and M.A.V. are Associates of the Howard Hughes Medical Institute.

Received: December 30, 2005
Revised: February 23, 2006
Accepted: March 31, 2006
Published: April 19, 2006

References

Allchorne, A.J., Broom, D.C., and Woolf, C.J. (2005). Detection of cold pain, cold allodynia and cold hyperalgesia in freely behaving rats. Mol. Pain *1*, 36.

Babes, A., Zorzon, D., and Reid, G. (2004). Two populations of cold-sensitive neurons in rat dorsal root ganglia and their modulation by nerve growth factor. Eur. J. Neurosci. *20*, 2276–2282.

Bandell, M., Story, G.M., Hwang, S.W., Viswanath, V., Eid, S.R., Petrus, M.J., Earley, T.J., and Patapoutian, A. (2004). Noxious cold ion channel TRPA1 is activated by pungent compounds and bradykinin. Neuron *41*, 849–857.

Bautista, D.M., Movahed, P., Hinman, A., Axelsson, H.E., Sterner, O., Hogestatt, E.D., Julius, D., Jordt, S.E., and Zygmunt, P.M. (2005). Pungent products from garlic activate the sensory ion channel TRPA1. Proc. Natl. Acad. Sci. USA *102*, 12248–12252.

Bautista, D.M., Jordt, S.E., Nikai, T., Tsuruda, P.R., Read, A.J., Poblete, J., Yamoah, E.N., Basbaum, A.I., and Julius, D. (2006). TRPA1 mediates the inflammatory actions of environmental irritants and proalgesic agents. Cell *124*, 1269–1282.

Berkley, K.J. (1997). Sex differences in pain. Behav. Brain Sci. *20*, 371–380.

Campbell, J.N., Raja, S.N., Meyer, R.A., and Mackinnon, S.E. (1988). Myelinated afferents signal the hyperalgesia associated with nerve injury. Pain *32*, 89–94.

Carlton, S.M., Lekan, H.A., Kim, S.H., and Chung, J.M. (1994). Behavioral manifestations of an experimental model for peripheral neuropathy produced by spinal nerve ligation in the primate. Pain *56*, 155–166.

Choi, Y., Yoon, Y.W., Na, H.S., Kim, S.H., and Chung, J.M. (1994). Behavioral signs of ongoing pain and cold allodynia in a rat model of neuropathic pain. Pain *59*, 369–376.

Clapham, D.E. (2003). TRP channels as cellular sensors. Nature *426*, 517–524.

Corey, D.P., and Hudspeth, A.J. (1980). Mechanical stimulation and micromanipulation with piezoelectric biomorph elements. J. Neurosci. Methods *3*, 183–202.

Corey, D.P., Garcia-Anoveros, J., Holt, J.R., Kwan, K.Y., Lin, S.Y., Vollrath, M.A., Amalfitano, A., Cheung, E.L., Derfler, B.H., Duggan, A., et al. (2004). TRPA1 is a candidate for the mechanosensitive transduction channel of vertebrate hair cells. Nature *432*, 723–730.

Craft, R.M., Mogil, J.S., and Aloisi, A.M. (2004). Sex differences in pain and analgesia. Eur. J. Pain *8*, 397–411.

Decosterd, I., and Woolf, C.J. (2000). Spared nerve injury: an animal model of persistent peripheral neuropathic pain. Pain *87*, 149–158.

Denk, W., Holt, J.R., Shepherd, G.M.G., and Corey, D.P. (1995). Calcium imaging of single stereocilia in hair cells: Localization of transduction channels at both ends of tip links. Neuron *15*, 1311–1321.

Fillingim, R.B., and Ness, T.J. (2000). Sex-related hormonal influences on pain and analgesic responses. Neurosci. Biobehav. Rev. *24*, 485–501.

Gale, J.E., Marcotti, W., Kennedy, H.J., Kros, C.J., and Richardson, G.P. (2001). FM1-43 dye behaves as a permeant blocker of the hair-cell mechanotransducer channel. J. Neurosci. *21*, 7013–7025.

Handwerker, H.O., Kilo, S., and Reeh, P.W. (1991). Unresponsive afferent nerve fibres in the sural nerve of the rat. J. Physiol. *435*, 229–242.

Hu, J., Milenkovic, H., and Lewin, G.R. (2006). The high threshold mechanotransducer: A status report. Pain *120*, 3–7.

Jaquemar, D., Schenker, T., and Trueb, B. (1999). An ankyrin-like protein with transmembrane domains is specifically lost after oncogenic transformation of human fibroblasts. J. Biol. Chem. *274*, 7325–7333.

Jordt, S.E., Bautista, D.M., Chuang, H.H., McKemy, D.D., Zygmunt, P.M., Hogestatt, E.D., Meng, I.D., and Julius, D. (2004). Mustard oils and cannabinoids excite sensory nerve fibres through the TRP channel ANKTM1. Nature *427*, 260–265.

Kachar, B., Parakkal, M., Kurc, M., Zhao, Y., and Gillespie, P.G. (2000). High-resolution structure of hair-cell tip links. Proc. Natl. Acad. Sci. USA *97*, 13336–13341.

Kobayashi, K., Fukuoka, T., Obata, K., Yamanaka, H., Dai, Y., Tokunaga, A., and Noguchi, K. (2005). Distinct expression of TRPM8, TRPA1, and TRPV1 mRNAs in rat primary afferent neurons with adelta/c-fibers and colocalization with trk receptors. J. Comp. Neurol. *493*, 596–606.

Koltzenburg, M., Lundberg, L.E., and Torebjork, H.E. (1992). Dynamic and static components of mechanical hyperalgesia in human hairy skin. Pain *51*, 207–219.

Koltzenburg, M., Torebjork, H.E., and Wahren, L.K. (1994). Nociceptor modulated central sensitization causes mechanical hyperalgesia in acute chemogenic and chronic neuropathic pain. Brain *117*, 579–591.

Lewin, G.R., and Mendell, L.M. (1993). Nerve growth factor and nociception. Trends Neurosci. *16*, 353–359.

Macpherson, L.J., Geierstanger, B.H., Viswanath, V., Bandell, M., Eid, S.R., Hwang, S., and Patapoutian, A. (2005). The pungency of garlic: activation of TRPA1 and TRPV1 in response to allicin. Curr. Biol. *15*, 929–934.

McKemy, D.D., Neuhausser, W.M., and Julius, D. (2002). Identification of a cold receptor reveals a general role for TRP channels in thermosensation. Nature *416*, 52–58.

McMahon, S.B., Armanini, M.P., Ling, L.H., and Phillips, H.S. (1994). Expression and coexpression of Trk receptors in subpopulations of adult primary sensory neurons projecting to identified peripheral targets. Neuron *12*, 1161–1171.

Meyers, J.R., MacDonald, R.B., Duggan, A., Lenzi, D., Standaert, D.G., Corwin, J.T., and Corey, D.P. (2003). Lighting up the senses: FM1–43 loading of sensory cells through nonselective ion channels. J. Neurosci. *23*, 4054–4065.

Molliver, D.C., Wright, D.E., Leitner, M.L., Parsadanian, A.S., Doster, K., Wen, D., Yan, Q., and Snider, W.D. (1997). IB4-binding DRG neurons switch from NGF to GDNF dependence in early postnatal life. Neuron *19*, 849–861.

Morin, C., and Bushnell, M.C. (1998). Temporal and qualitative properties of cold pain and heat pain: a psychophysical study. Pain *74*, 67–73.

Obata, K., Katsura, H., Mizushima, T., Yamanaka, H., Kobayashi, K., Dai, Y., Fukuoka, T., Tokunaga, A., Tominaga, M., and Noguchi, K. (2005). TRPA1 induced in sensory neurons contributes to cold hyperalgesia after inflammation and nerve injury. J. Clin. Invest. *115*, 2393–2401.

Patapoutian, A., Peier, A.M., Story, G.M., and Viswanath, V. (2003). ThermoTRP channels and beyond: mechanisms of temperature sensation. Nat. Rev. Neurosci. *4*, 529–539.

Peier, A.M., Moqrich, A., Hergarden, A.C., Reeve, A.J., Andersson, D.A., Story, G.M., Earley, T.J., Dragoni, I., McIntyre, P., Bevan, S., and Patapoutian, A. (2002). A TRP channel that senses cold stimuli and menthol. Cell *108*, 705–715.

Pertin, M., Ji, R.R., Berta, T., Powell, A.J., Karchewski, L., Tate, S.N., Isom, L.L., Woolf, C.J., Gilliard, N., Spahn, D.R., and Decosterd, I. (2005). Upregulation of the voltage-gated sodium channel β2 subunit in neuropathic pain models: characterization of expression in injured and non-injured primary sensory neurons. J. Neurosci. *25*, 10970–10980.

Ramakers, C., Ruijter, J.M., Deprez, R.H., and Moorman, A.F. (2003). Assumption-free analysis of quantitative real-time polymerase chain reaction (PCR) data. Neurosci. Lett. *339*, 62–66.

Reeh, P.W., Kocher, L., and Jung, S. (1986). Does neurogenic inflammation alter the sensitivity of unmyelinated nociceptors in the rat? Brain Res. *384*, 42–50.

Reid, G. (2005). ThermoTRP channels and cold sensing: what are they really up to? Pflugers Arch. *451*, 250–263.

Rosenzweig, M., Brennan, K.M., Tayler, T.D., Phelps, P.O., Patapoutian, A., and Garrity, P.A. (2005). The Drosophila ortholog of vertebrate TRPA1 regulates thermotaxis. Genes Dev. *19*, 419–424.

Rüsch, A., and Eatock, R.A. (1996). A delayed rectifier conductance in type I hair cells of the mouse utricle. J. Neurophysiol. *76*, 995–1004.

Simpson, E.M., Linder, C.C., Sargent, E.E., Davisson, M.T., Mobraaten, L.E., and Sharp, J.J. (1997). Genetic variation among 129 substrains and its importance for targeted mutagenesis in mice. Nat. Genet. *16*, 19–27.

Story, G.M., Peier, A.M., Reeve, A.J., Eid, S.R., Mosbacher, J., Hricik, T.R., Earley, T.J., Hergarden, A.C., Andersson, D.A., Hwang, S.W., et al. (2003). ANKTM1, a TRP-like channel expressed in nociceptive neurons, is activated by cold temperatures. Cell *112*, 819–829.

Suter, M.R., Papaloizos, M., Berde, C.B., Woolf, C.J., Gilliard, N., Spahn, D.R., and Decosterd, I. (2003). Development of neuropathic pain in the rat spared nerve injury model is not prevented by a peripheral nerve block. Anesthesiology *99*, 1402–1408.

Tracey, W.D., Jr., Wilson, R.I., Laurent, G., and Benzer, S. (2003). *painless*, a *Drosophila* gene essential for nociception. Cell *113*, 261–273.

Viswanath, V., Story, G.M., Peier, A.M., Petrus, M.J., Lee, V.M., Hwang, S.W., Patapoutian, A., and Jegla, T. (2003). Opposite thermosensor in fruitfly and mouse. Nature *423*, 822–823.

Vollrath, M.A., and Eatock, R.A. (2003). Time course and extent of mechanotransducer adaptation in mouse utricular hair cells: comparison with frog saccular hair cells. J. Neurophysiol. *90*, 2676–2689.

Walker, R.G., Willingham, A.T., and Zuker, C.S. (2000). A Drosophila mechanosensory transduction channel. Science *287*, 2229–2234.

Zimmermann, M. (1983). Ethical guidelines for investigations of experimental pain in conscious animals. Pain *16*, 109–110.